

Potential Problems by Singular Boundary Method Satisfying Moment Condition

Wen Chen^{1,2}, Zhuojia Fu¹ and Xing Wei¹

Abstract: This study investigates the singular boundary method (SBM), a novel boundary-type meshless method, in the numerical solution of potential problems. Our finding is that the SBM can not obtain the correct solution in some tested cases, in particular, in the cases whose solution includes a constant term. To remedy this drawback, this paper presents an improved SBM formulation which is a linear sum of the fundamental solution adding in a constant term. It is stressed that this SBM approximation with the additional constant term has to satisfy the so-called moment condition in order to guarantee the uniqueness of the solution. The efficiency and accuracy of the present SBM scheme are demonstrated through detailed comparisons with the exact solution, the method of fundamental solutions and the regularized meshless method.

Keywords: Singular boundary method, fundamental solution, singularity at the origin, moment condition, potential problem

1 Introduction

Without a need of harassing mesh generation in the traditional FEM [Zienkiewicz and Taylor (1991)] and BEM [Ong and Lim (2005)], meshless methods [Li and Liu (2002)] have attracted much attention in recent years. This study focuses on the boundary-type meshless numerical techniques, for instance, method of fundamental solutions (MFS) [Chen, Golberg and Hon (1998); Cheng, Young and Tsai (2000); Fairweather and Karageorghis (1998); Karageorghis (1992); Liu (2008); Marin (2008,2010a,2010b); Poullikkas, Karageorghis and Georgiou (1998); Reutskiy (2005); Smyrlis and Karageorghis (2001)], boundary knot method (BKM) by Chen and Tanaka (2002), boundary particle method [Chen and Fu (2009): Fu, Chen

¹ Center for Numerical Simulation Software in Engineering and Sciences, Department of Engineering Mechanics, College of Civil Engineering, Hohai University, Nanjing, Jiangsu, P.R.China

² Corresponding author. E-mail: chenwen@hhu.edu.cn. Department of Engineering Mechanics, Hohai University, Xikang Road #1, Nanjing City, Jiangsu Province, 210098, P.R.China

and Yang (2009); Fu and Chen (2009)], collocation Trefftz method (CTM) by Liu (2007a, 2009), meshless regularized integral equation method by Liu (2007b, 2007c), boundary collocation method (BCM) by Chen, Chang, Chen and Lin (2002), regularized meshless method (RMM) [Chen, Kao, Chen, Young and Lu (2006); Young, Chen and Lee (2005); Young, Chen, Chen and Kao (2007); Chen, Kao and Chen (2009); Song and Chen (2009)], modified method of fundamental solution (MMFS) by Sarler (2008) and Meshless Local Petrov-Galerkin (MLPG) method by [Atluri, Liu and Han (2006); Han and Atluri (2004); Sladek, Sladek and Atluri (2004)].

The MFS has been widely applied to some engineering and science problems, whose approximate solution is expressed as a linear combination of fundamental solutions of the governing equation of interest. To avoid the singularity of the fundamental solution, the method distributes the source nodes on a fictitious boundary outside the physical domain. The location of such a fictitious boundary is vital to the accuracy of the solution. Its placement, however, is still an opening issue and largely problem-dependent.

Instead of using the singular fundamental solution, the nonsingular general solution is employed to evaluate the homogeneous solutions in the BKM and BCM. These methods place the interpolation knots on the real boundary. But the drawback of the ill-condition matrices occurs with a medium number of nodes. This may jeopardize the accuracy of the numerical results. And the appropriate nonsingular general solutions may not be found in some cases. For instance, the Laplace equation has no nonsingular general solution. To remedy this problem, the different schemes have been proposed, for example, employing the translate-invariant 2D Laplacian harmonic function proposed by Hon and Wu (2000) or the nonsingular general solutions of Helmholtz or modified Helmholtz operators proposed by Chen, Shen, Shen and Yuan (2005). However, the accuracy of these approaches depends on an artificial parameter, which is problem-dependent.

By employing the desingularization of subtracting and adding-back technique, Young, Chen and Lee (2005) proposed an alternative meshless method, namely, regularized meshless method (RMM) [Chen, Kao, Chen, Young and Lu (2006); Young, Chen, Chen and Kao (2007)]. Like the BKM and BCM, the RMM also places the source points on the real physical boundary to circumvent the fictitious boundary of the MFS. In addition, the RMM also circumvents the ill-conditioned interpolation matrix of the MFS, BKM, and BCM. However, the original RMM requires uniform distribution of nodes and severely reduces its applicability. Similar to the RMM, Sarler (2008) proposes the modified method of fundamental solution (MMFS) to solve potential flow problems. However, the MMFS demands a complex calculation of the diagonal elements of interpolation matrix.

Chen (2009) recently proposed a novel numerical method, called the singular bound-

ary method (SBM). The SBM is mathematically simple, easy-to-program, accurate, meshless and integration-free and avoids the controversy of the fictitious boundary in the MFS and the uniform boundary node requirement of the RMM and the expensive calculation of diagonal elements in the MMFS. However, we find that the SBM performs well for some tested problems but that it can result in the wrong solution of the other problems, especially for the problem whose solution includes a constant potential.

In order to remedy this drawback, this paper proposes an improved singular boundary method, which will be introduced in Section 2. The key procedure of the SBM is the inverse interpolation technique (IIT) which avoids the singularity of the fundamental solution at the origin. In Section 3, this paper presents an improved SBM formulation which satisfies the moment condition. Section 4 examines the efficiency, accuracy and convergence of the improved SBM to the potential problems in different boundary-shape domains. Finally, Section 5 concludes this paper with some remarks.

2 Original singular boundary method

This section introduces the singular boundary method (SBM) for Laplace problem. Consider the Laplace equation:

$$\nabla^2 u(x) = 0 \quad x \in \Omega \quad (1)$$

subjected to boundary conditions:

$$\begin{aligned} u(x) &= \bar{u} \quad x \in \Gamma_D \\ q(x) &= \bar{q} \quad x \in \Gamma_N \end{aligned} \quad (2)$$

where ∇^2 denotes the Laplacian operator, the solutions $u(x)$ is the potentials in the fields of electromagnetism, astronomy, and fluid dynamics, Ω denotes the physical domain. $q(x) = \frac{\partial u(x)}{\partial n}$, n the unit outward normal on the physical boundary. Γ_D, Γ_N are the Dirichlet boundary (essential boundary) and Neumann boundary (natural boundary) parts, respectively, which construct the whole boundary of the physical domain Ω .

By adopting the fundamental solution G of Laplace equation, the solution $u(x)$ is approximated by a linear combination of fundamental solutions with respect to different source points s_j as below:

$$u(x) = \sum_{j=1}^N \alpha_j G(x, s_j) \quad (3)$$

where N is the number of source points, α_j is the j th unknown coefficient.

In the MFS, the fundamental solution G has no singularities because of the source points distributed on the fictitious boundary, which locates outside the physical domain. It can be expressed as follows:

$$G(x, s_j) = \begin{cases} -\frac{1}{2\pi} \ln(\|x - s_j\|_2) & x \in R^2 \\ \frac{1}{4\pi\|x - s_j\|_2} & x \in R^3 \end{cases} \quad (4)$$

The fundamental solution can be applied to both interior and exterior problems. However, despite of great effort of 40 years, the placement of the fictitious boundary in the MFS remains a perplexing issue when dealing with complex-shaped boundary or multiply-connected domain problems.

In this study, we place all computing nodes on the same physical boundary, and the source points s_j and the collocation points x_i are the same set of boundary nodes. By employing a novel inverse interpolation technique (IIT), we regularize the singularity of the fundamental solution upon the coincidence of the source and collocation points. It is noted that the singularity occurs at the calculation of the diagonal terms of the interpolation matrix. The SBM formulation is given by

$$u(x_i) = \sum_{j=1}^N \alpha_j G_S(x_i, s_j) \quad (5)$$

in which

$$G_S(x_i, s_j) = \begin{cases} G_{ii} & x_i = s_j, x_i \in \Gamma_D \cup \Omega \\ G(x_i, s_j) & x_i \neq s_j, x_i \in \Gamma_D \cup \Omega \end{cases} \quad (6)$$

$$\frac{\partial G_S(x_i, s_j)}{\partial n} = \begin{cases} \bar{G}_{ii} & x_i = s_j, x_i \in \Gamma_N \\ \frac{\partial G(x_i, s_j)}{\partial n} & x_i \neq s_j, x_i \in \Gamma_N \end{cases} \quad (7)$$

where G_{ii} and \bar{G}_{ii} are defined as the source intensity factors, namely, the diagonal elements of the SBM interpolation matrix. This study employs a simple numerical technique, called the inverse interpolation technique (IIT), to determine the source intensity factors. In the first step, the IIT requires choosing a known sample solution u_I of the Laplace potential problem and locating some sample points y_k inside the physical domain. It is noted that the sample points y_k do not coincide with the source points s_i , and the sample points number M should not be fewer than the physical boundary source node number N . By using the interpolation formula (3),

we can then determine the influence coefficients β_j by the following linear equations

$$\{G(y_k, s_j)\} \{\beta_j\} = \{u_I(y_k)\} \quad (8)$$

Replacing the sample points y_k with the boundary collocation points x_i and inserting the influence coefficients β_j determined from Eq. (8), the SBM interpolation matrix of potential problem (Eqs. (1) and (2)) can be written as

$$\left\{ \begin{matrix} G_S(x_i, s_j) \\ \frac{\partial G_S(x_i, s_j)}{\partial n} \end{matrix} \right\} \{\beta_j\} = \left\{ \begin{matrix} u_I(x_i) \\ \frac{\partial u_I(x_i)}{\partial n} \end{matrix} \right\} \quad (9)$$

It is noted that only the source intensity factors G_{ii} and \bar{G}_{ii} are unknown in the above equation (9), hence the source intensity factors can be calculated by the following formulations:

$$G_{ii} = \frac{u_I(x_i) - \sum_{j=1, s_j \neq x_i}^N \beta_j G(x_i, s_j)}{\beta_j} \quad x_i = s_j, \quad x_i \in \Gamma_D \quad (10)$$

$$\bar{G}_{ii} = \frac{\frac{\partial u_I(x_i)}{\partial n} - \sum_{j=1, s_j \neq x_i}^N \beta_j \frac{\partial G(x_i, s_j)}{\partial n}}{\beta_j} \quad x_i = s_j, \quad x_i \in \Gamma_N \quad (11)$$

It is stressed that the source intensity factors only depends on the distribution of the source points, the fundamental solution of the governing equation and the boundary conditions. Theoretically speaking, the source intensity factors remain unchanged with different sample solutions with the IIT. Therefore, by employing a novel inverse interpolation technique, we circumvent the singularity of the fundamental solution upon the coincidence of the source and collocation points.

According to our numerical experiments, for an uniform distribution of source points along a circular physical boundary, the source intensity factors G_{ii} and \bar{G}_{ii} calculated by the inverse interpolation technique (IIT) is very close to the sum of the off-diagonal elements of the interpolation matrix, called the sum technique (ST) in this paper, namely,

$$G_{ii} = - \sum_{j=1, s_j \neq x_i}^N G(x_i, s_j) \quad x_i = s_j, \quad x_i \in \Gamma_D \quad (12)$$

$$\bar{G}_{ii} = \sum_{j=1, s_j \neq x_i}^N \frac{\partial G(x_i, s_j)}{\partial n} \quad x_i = s_j, \quad x_i \in \Gamma_N \quad (13)$$

To verify the availability of the above two approaches, an interior Dirichlet problem in circular domain has been calculated. In the numerical approach, the sample solution $u_I = x + y$ and the sample point number M is 400. It is stressed that the sample points can be collocated at arbitrary location, except for superposition with the source points. In this paper, the sample point is placed along an inner boundary analogous to the physical boundary. Fig.1 illustrates the location of the collocation, source and sample points. Fig.2a shows that two expressions (10) and (11) have the similar results. Fig.2b displays that the source intensity factors remain unchanged with three different sample solutions: (a) $u_I = x + y$, (b) $u_I = x^2 - y^2$, (c) $u_I = e^x \cos y$.

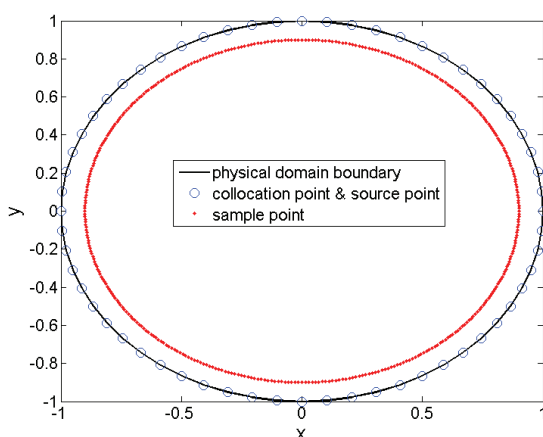


Figure 1: The distribution of collocation, source and sample points in the SBM.

However when the distribution of source points is nonuniform on a circular boundary or the physical domain is not a circle, the sum technique fails to evaluate correct value of the source intensity factors.

3 Improved singular boundary method

The SBM formulation (4) performs well for some problems. But we also find that it can result in the wrong solution of the other problems, especially for the problem whose solution includes a constant potential. In order to remedy this drawback, we add a constant term to the SBM formulation (4) to guarantee the uniqueness of the SBM interpolation matrix. The improved SBM formulation with a constant term is

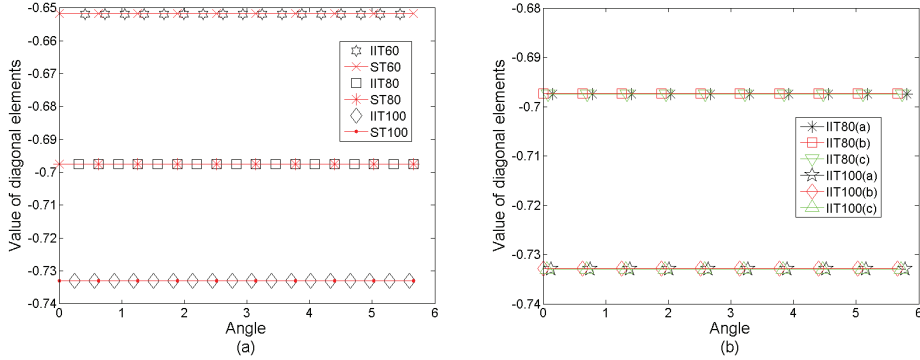


Figure 2: The source intensity factor G_{ii} of an uniform distribution of circular boundary nodes by using (a) the inverse interpolation technique (see Eq. (10)) and the sum technique (see Eq. (11)) with various numbers of source points ($N=60,80,100$); (b) the inverse interpolation technique with different sample solutions using 80 and 100 source points.

given by

$$u(x) = \sum_{j=1}^N \alpha_j G_S(x, s_j) + \alpha_{N+1} \quad (14)$$

with the constraint

$$\sum_{j=1}^N \alpha_j = 0. \quad (15)$$

This technique is also called as moment condition in Chen, Hon and Schaback (2009). The efficiency and accuracy of the improved SBM (ISBM) solving the potential problems includes a constant potential are demonstrated in the following section.

4 Numerical results

In this section, the efficiency, accuracy and convergence of the improved SBM are tested to the potential problems with circular, square and irregular domains, subjected to the various boundary conditions. It is stressed that the boundary conditions are discontinuous in the two cases. The performances of the ISBM are compared with that of the RMM and the MFS. In this study, only the double layer potentials are chosen in RMM.

$Rerr(u)$ represents the average relative error and $Merr(u)$ is the maximum absolute error, which are defined by

$$Rerr(u) = \sqrt{\frac{1}{NT} \sum_{i=1}^{NT} \left| \frac{u(i) - \bar{u}(i)}{\bar{u}(i)} \right|^2}, \quad (16)$$

$$Merr(u) = \max_{1 \leq i \leq NT} |u(i) - \bar{u}(i)|, \quad (17)$$

where $\bar{u}(i)$ and $u(i)$ are the analytical and numerical solutions at x_i , respectively, and NT denotes the total number of points in the interest domain, which are used to test the solution accuracy. Unless otherwise specified, NT is taken to be 2209 for square domain problems and 1010 for circular domain problems in all following numerical cases. In the first two circular domain problems, the ST technique in Eq. (11) has been employed. And in the next three examples, the IIT technique in Eq. (10) has been employed, where the sample solution is $u_I = x + y$ and the sample point number $M = 400$.

Example 1: This case compares the original SBM and the improved SBM in the solution of a circular domain Laplace problem.

The exact solution is given by

$$u(x, y) = e^y (\sin(x) + \cos(x)) \quad (18)$$

and the problem is subjected to Dirichlet boundary condition, which can easily be derived accordingly. We find that the original SBM yields the wrong solution. In contrast, the improved SBM produces the correct solution.

By using 100 boundary nodes, its average relative error is $Rerr(u)=3.53e-05$ and the maximum absolute error is $Merr(u)= 3.34e-05$. Fig. 3 displays the contour plot of the improved SBM and the exact solutions. It can be found from Fig. 3 that the improved SBM numerical solution agrees very well with the exact solution.

Example 2: The Dirichlet problem with circular domain

The problem is subjected to discontinuous Dirichlet boundary condition as follows:

$$u(1, \theta) = \begin{cases} 1 & 0 < \theta < \pi \\ 2 & \pi < \theta < 2\pi \end{cases} \quad (19)$$

The exact solution is given by

$$u(x, y) = \frac{1}{\pi} \arctan \left(\frac{1 - x^2 - y^2}{2y} \right) + 1 \quad (20)$$

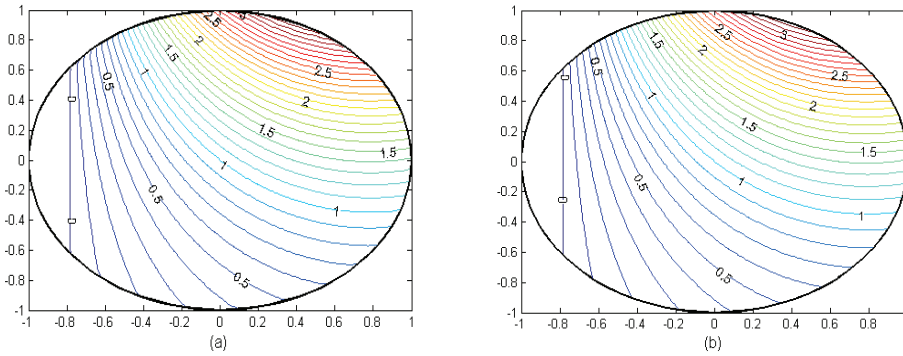


Figure 3: (a) The improved SBM solution and (b) the exact solution for Example 1.

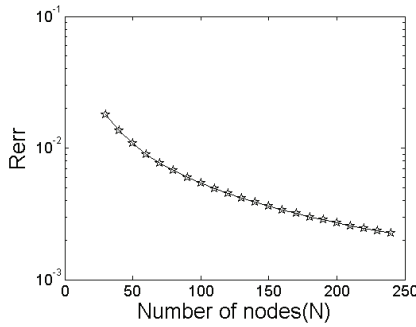


Figure 4: The average relative errors ($Rerr$) with respect to the boundary node number (N) in Example 2

Fig.4 shows numerical accuracy of the improved SBM with respect to the boundary collocation point number N . The average relative error $Rerr$ decreases with increasing boundary points. Comparison is made with the analytical solution, the RMM and MFS solutions. The contour plot of the exact solution is plotted in Fig.5. Figs. 6-8 illustrate the field solutions by the improved singular boundary method (ISBM), the RMM and the MFS ($R=1.3$) with 100 boundary nodes, respectively. It is observed that the results of the ISBM and the MFS agree very well with the exact solution. Comparing Figs. 5 and 7, we can find that the RMM results at the region adjacent to boundary are clearly larger than the exact solution.

Table 1 shows the numerical comparison between the ISBM and the RMM. And the

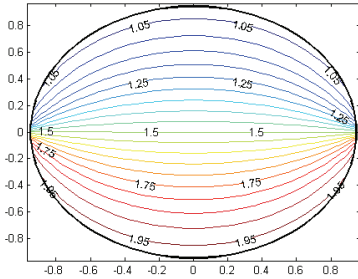


Figure 5: The exact solution for Example 2

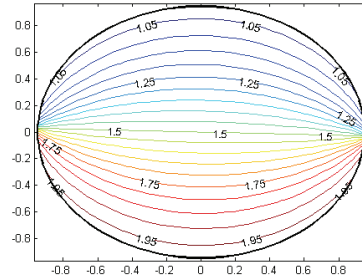


Figure 6: The field solution for Example 2 by using ISBM

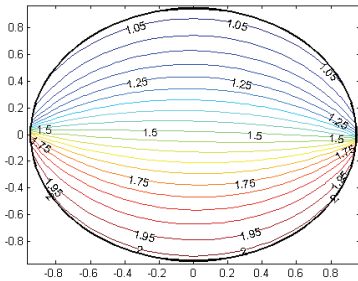
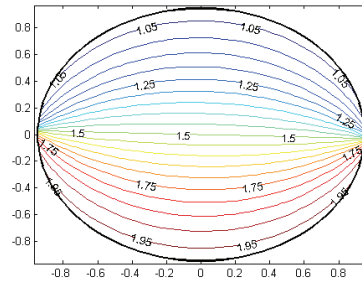


Figure 7: The field solution for Example 2 by using RMM

Figure 8: The field solution for Example 2 by using MFS($R=1.3$)

results of the MFS with different off-set boundary are shown in Table 2. Where the condition number $Cond$ is defined as the ratio between the largest and smallest singular value. We can see from Table 2 that the numerical accuracy of the MFS with the off-set boundary radius $R = 3$ is best among all numerical methods. However, the MFS results are wrong with the off-set boundary radius $R = 1$. This illustrates the location of source points is vital to the MFS numerical accuracy. Thanks to the IIT, the present scheme avoids such a difficulty in choosing an optimal off-set boundary. The RMM also circumvents the fictitious boundary in the MFS. And the errors of the present method are less than the RMM, whereas its condition number is a little larger than the RMM.

Example 3: The Dirichlet problem with square domain

We investigate a square domain (1×1) with the Dirichlet discontinuous boundary

Table 1: Numerical results (ISBM and RMM) for Example 2 with various numbers of nodes.

N	Improved SBM			RMM		
	Rerr(u)	Merr(u)	Cond(A)	Rerr(u)	Merr(u)	Cond(A)
80	9.00E-03	1.16E-01	4.05E+01	1.54E-02	1.41E-01	2.03E+00
100	7.20E-03	9.36E-02	4.53E+01	1.23E-02	1.12E-01	2.02E+00
200	3.60E-03	4.73E-02	7.21E+01	6.10E-03	5.54E-02	2.01E+00

Table 2: Numerical results (MFS) for Example 2 with various numbers of nodes.

N	MFS(R=3)			MFS(R=1.3)		
	Rerr(u)	Merr(u)	Cond(A)	Rerr(u)	Merr(u)	Cond(A)
80	8.90E-03	1.11E-01	1.84E+18	9.00E-03	1.17E-01	5.56E+05
100	7.01E-02	2.01E-01	3.91E+18	7.20E-03	9.42E-02	9.58E+06
200	3.50E-03	4.45E-02	1.37E+20	3.60E-03	4.74E-02	9.54E+12

conditions as follows:

$$u(x, 0) = x + 2, u(x, 1) = u(0, y) = u(1, y) = 2 \tag{21}$$

The analytical solution of this problem is given by

$$u(x, y) = 2 + \sum_{n=1}^{\infty} \frac{2(-1)^n}{n\pi \sinh(n\pi)} \sinh(n\pi(1 - y)) \sin(n\pi x) \tag{22}$$

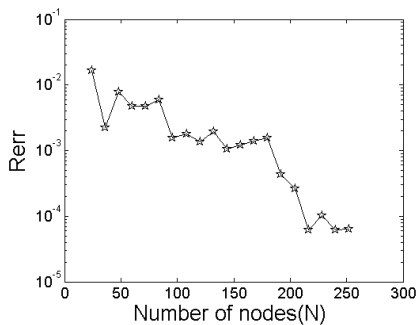


Figure 9: The average relative errors (*Rerr*) with respect to the boundary node number (*N*) in Example 3

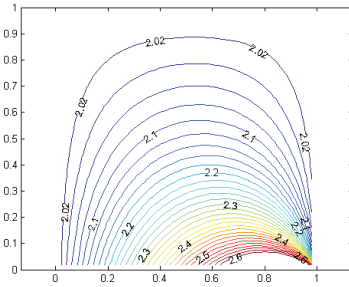


Figure 10: The exact solution for Example 3

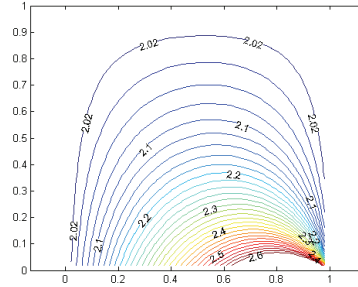


Figure 11: The field solution for Example 3 by using ISBM

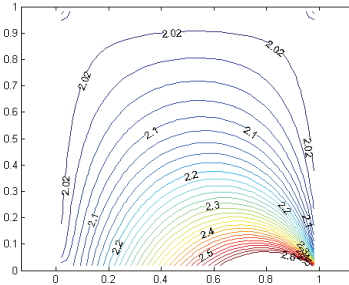


Figure 12: The field solution for Example 3 by using RMM

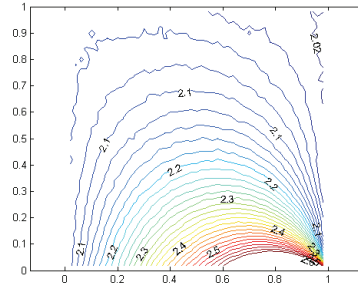


Figure 13: The field solution for Example 3 by using MFS(R=1.5)

Table 3: Numerical results (ISBM and RMM) for Example 3 with various numbers of nodes.

N	Improved SBM			RMM		
	Rerr(u)	Merr(u)	Cond(A)	Rerr(u)	Merr(u)	Cond(A)
28	8.30E-03	3.37E-01	2.84E+01	1.21E-01	1.44E+00	1.17E+01
40	2.50E-03	1.44E-01	5.82E+01	6.91E-02	9.30E-01	8.69E+00
100	2.30E-03	5.47E-02	6.28E+05	1.42E-02	1.09E-01	4.90E+00
120	1.40E-03	3.42E-02	2.13E+06	9.30E-03	6.46E-02	4.67E+00
200	1.00E-03	5.80E-02	5.60E+02	3.72E-04	1.13E-02	4.39E+00
240	6.26E-05	3.90E-03	1.72E+02	2.50E-03	2.67E-02	4.34E+00

Fig.9 displays the numerical accuracy of the ISBM against the number of boundary nodes, and we can find that the accuracy enhances with the increasing boundary

Table 4: Numerical results (MFS) for Example 3 with various numbers of nodes.

N	MFS(R=2)			MFS(R=1.5)		
	Rerr(u)	Merr(u)	Cond(A)	Rerr(u)	Merr(u)	Cond(A)
28	1.17E-02	1.57E-01	3.96E+08	1.17E-02	1.57E-01	4.13E+06
40	6.80E-03	9.88E-02	1.11E+17	6.20E-03	8.80E-02	3.48E+17
100	1.36E-02	4.72E-02	5.48E+18	1.06E-02	7.36E-02	1.40E+19
120	6.53E-02	2.27E-01	5.77E+19	1.01E-02	5.65E-02	1.89E+19
200	3.30E-03	3.66E-02	1.09E+19	1.29E-02	6.47E-02	1.12E+19
240	2.59E-02	1.25E-01	5.88E+19	1.72E-02	5.70E-02	1.43E+19

node number N . The contour plot of the exact solution is plotted in Fig. 10. Figs. 11-13 displays the field solutions of the ISBM, the RMM and the MFS ($R=1.5$) with 160 boundary nodes, respectively. It is observed that the ISBM results agree well with the exact solution very well. The numerical results at the region adjacent to boundary by the RMM deteriorate significantly compared with those in central region. It is noted that the MFS does not yield reliable and consistent solution.

Table 3 shows the results by the ISBM and the RMM. The numerical accuracy by the ISBM with 28 boundary nodes is comparable with that of the RMM with 120 boundary nodes. Table 4 shows the MFS results with different off-set boundary. There is much oscillation with the increasing boundary node number N by the MFS, and the culprit of this accuracy variation is the ill-conditioned interpolation matrix.

Example 4: The mixed-type problem with square domain

We consider a square domain (1×1) with the mixed-type BC:

$$u(x, 0) = x^2 + 1, u(x, 1) = x^2, u_y(0, y) = u_y(1, y) = -2y \tag{23}$$

The exact solution is given by

$$u(x, y) = x^2 - y^2 + 1 \tag{24}$$

The contour plot of the exact solution is plotted in Fig.14. Figs. 15 and 16 depict the field solutions obtained by the ISBM and RMM with 100 boundary nodes, respectively. It is observed that the ISBM results match the exact solution very well. The numerical results nearby boundary corners by the RMM deteriorate notably.

Table 5 presents the numerical results of the improved SBM and the RMM with various numbers of boundary nodes. The numerical accuracy by the ISBM with 40 nodes is equally well to the RMM with 200 nodes. In addition, the MFS can suffice extreme accuracy with few nodes in this case.

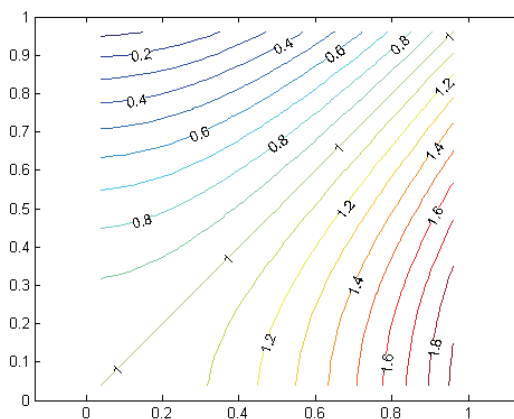


Figure 14: The exact solution for Example 4

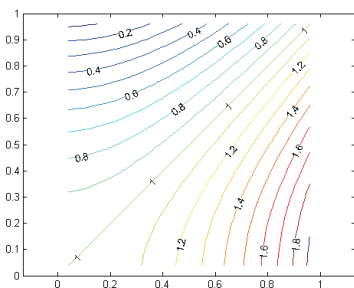


Figure 15: The field solution for Example 4 by using ISBM

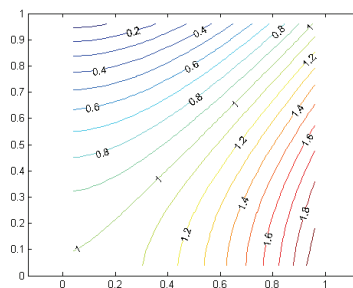


Figure 16: The field solution for Example 4 by using RMM

Example 5: The Dirichlet problem with irregular domain in Chen, Shen, Shen and Yuan (2005).

We test an irregular domain problem with the Dirichlet boundary condition:

$$u(x,y) = e^x \cos y + 3 \quad (x,y) \in B \quad (25)$$

The exact solution is given by

$$u(x,y) = e^x \cos y + 3 \quad (26)$$

Table 5: Numerical results (ISBM and RMM) for Example 4 with various numbers of nodes.

N	Improved SBM			RMM		
	Rerr(u)	Merr(u)	Cond(A)	Rerr(u)	Merr(u)	Cond(A)
28	2.78E-02	6.33E-02	1.02E+03	2.75E-01	1.12E+00	3.85E+02
40	5.00E-03	1.20E-02	1.42E+02	1.69E-01	8.45E-01	2.77E+02
100	2.02E-02	5.88E-02	1.58E+05	3.69E-02	1.36E-01	1.27E+02
200	4.71E-04	8.80E-04	1.54E+02	4.70E-03	2.46E-02	1.03E+02
240	2.12E-04	9.01E-04	2.40E+02	9.10E-03	4.41E-02	1.21E+02

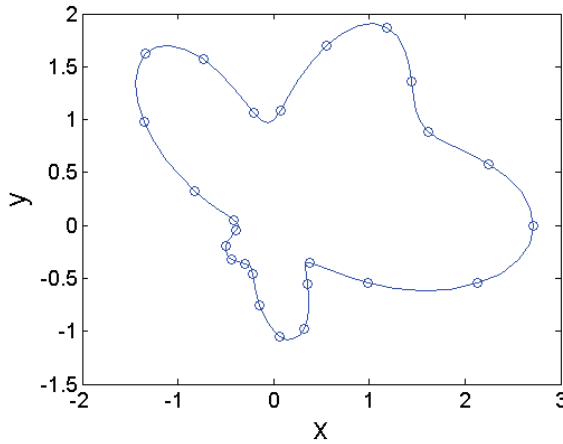


Figure 17: The shape of irregular domain for Example 5 and collocation nodes

Fig.17 shows the configuration of irregular domain and boundary collocation points, denoted by a small circle. The contour plot of the exact solution is plotted in Fig.18. Fig.19 depicts the ISBM field solutions with 150 boundary nodes. It is observed that the improved SBM results match the exact solutions very well. Table 6 shows that the numerical accuracy by the present SBM becomes more accurate with increasing boundary nodes.

Example 6: The Dirichlet problem with L-shaped domain.

We investigate the present SBM in L-shaped domain problem with the exact solution:

$$u(x,y) = \sinh(x) \cos(y) + 2 \tag{27}$$

Fig.20 shows the configuration of L-shaped domain and the distribution of bound-

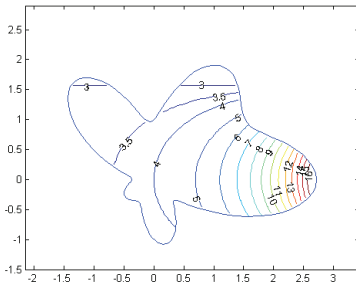


Figure 18: The exact solution for Example 5

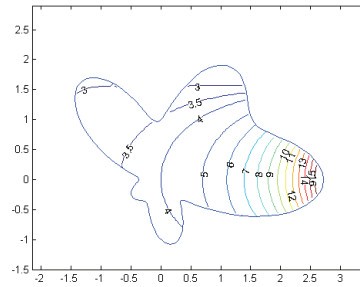


Figure 19: The field solution for Example 5 by using ISBM

Table 6: Numerical results of ISBM for Example 5 with various numbers of nodes.

N	Improved SBM		
	Rerr(u)	Merr(u)	Cond(A)
30	2.10E-02	8.23E-01	5.16E+01
80	3.70E-03	4.13E-01	6.09E+01
100	2.60E-03	4.41E-01	6.09E+01
150	1.80E-03	3.00E-01	6.06E+02
200	2.70E-03	2.46E-01	1.03E+05
400	4.70E-04	5.63E-02	5.72E+10

any collocation points, denoted by a small circle. Fig.21 plots the contour plot of the exact solution. Fig.22 depicts the ISBM field solutions with 160 boundary nodes. It can be found from Fig. 21 and 22 that the improved SBM results match the exact solutions very well. Table 7 shows that the numerical accuracy enhances with increasing boundary nodes by the present SBM. This example verifies that the proposed method works equally well in physical domain with boundary singularities.

5 Conclusions

In this paper, we present an improved singular boundary method, which uses the inverse interpolation technique to circumvent the singularity of the fundamental solution at the origin. Moreover, we add a constant term to guarantee the uniqueness of the SBM numerical solution, especially when the problem of interest includes a constant solution.

The numerical results in Section 4 reveal that the improved SBM is a competitive

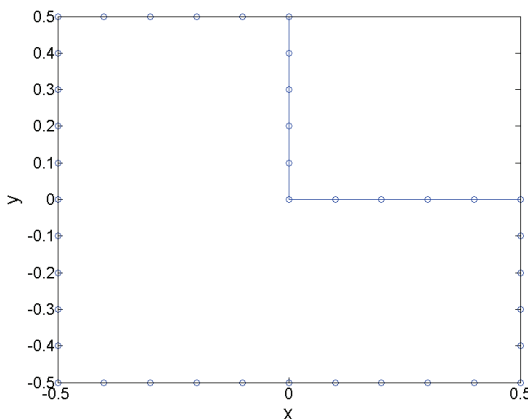


Figure 20: The configuration of L-shaped domain in Example 6 and collocation nodes

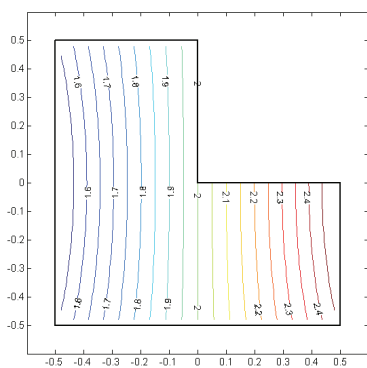


Figure 21: The exact solution for Example 6

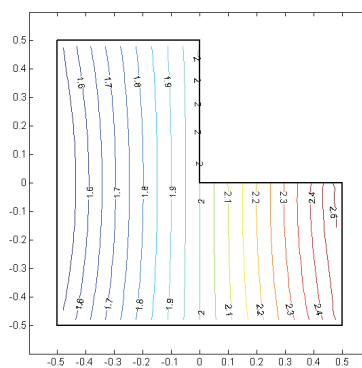


Figure 22: The field solution for Example 6 by using ISBM

boundary collocation method to solve the Laplace problems with arbitrary domains. Like the method of fundamental solution, regularized meshless method, and modified method of fundamental solution, the ISBM is mathematically simple, easy-to-program, meshless and integration-free. On the other hand, the ISBM avoids the fictitious boundary and the ill-conditioned interpolation matrix of the MFS and outperforms the MFS in solution of discontinuous boundary condition problems. Compared with the RMM, the ISBM has better accuracy with the same number of boundary nodes and avoids the uniform boundary node requirement. The evalua-

Table 7: Numerical results of ISBM for Example 6 with various numbers of nodes.

N	Improved SBM		
	Rerr(u)	Merr(u)	Cond(A)
24	6.30E-03	7.69E-02	5.10E+01
40	1.90E-03	3.37E-02	6.03E+01
120	1.80E-03	2.76E-02	3.74E+04
160	1.30E-03	2.25E-02	2.46E+04
240	7.11E-04	2.09E-02	6.54E+04
320	5.69E-04	1.55E-02	2.10E+07

tion of diagonal elements in the ISBM is far more simple and efficient than in the MMFS.

Acknowledgement: The work described in this paper was supported by National Basic Research Program of China (973 Project No. 2010CB832702) and Natural Science Foundation of Hohai University (Grant No. 409251). And the second author would like to thank China Scholarship Council (CSC) for the financial support.

References

- Atluri, S. N.; Liu, H. T.; Han, Z. D.** (2006): Meshless Local Petrov-Galerkin (MLPG) mixed collocation method for elasticity problems. *CMES: Computer Modeling in Engineering & Sciences*, vol.14, pp.141-152
- Chen, C. S.; Golberg, M. A.; Hon, Y. C.** (1998): The method of fundamental solutions and quasi-Monte-Carlo method for diffusion equations. *International Journal for Numerical Methods in Engineering*, vol. 43, pp. 1421-1435
- Chen, C. S.; Hon, Y. C.; Schaback, R. S.** (2009): Radial Basis Functions with Scientific Computation, under review.
- Chen, W.; Tanaka, M.** (2002): A meshless, exponential convergence, integration-free, and boundary-only RBF technique. *Computers & Mathematics with Applications*, vol. 43, pp. 379-391
- Chen, W.; Shen, L. J.; Shen, Z. J.; Yuan, G. W.** (2005): Boundary knot method for Poisson equations. *Engineering Analysis with Boundary Elements*, vol. 29(8), pp. 756-760
- Chen, W.** (2009): Singular boundary method: A novel, simple, mesh-free, boundary collocation numerical method. *Acta Mechanica Solida Sinica*, (in Chinese) to

be published.

Chen, W.; Fu, Z. J. (2009): Boundary particle method for inverse Cauchy problems of the inhomogeneous Helmholtz equations. *Journal of Marine Science and Technology*, vol. 17(3), pp. 157-163

Chen, J. T.; Chang, M. H.; Chen, K. H.; Lin, S. R. (2002): The boundary collocation method with meshless concept for acoustic eigenanalysis of two-dimensional cavities using radial basis function. *Journal of Sound and Vibration*, vol. 257, pp. 667-711

Chen, K. H.; Kao, J. H.; Chen, J. T.; Young, D. L.; Lu, M. C. (2006): Regularized meshless method for multiply-connected-domain Laplace problems. *Engineering Analysis with Boundary Elements*, vol. 30, pp. 882-896

Chen, K.H.; Kao, J.H.; Chen, J.T. (2009): Regularized meshless method for antiplane piezoelectricity problems with multiple inclusions. *CMC: Computers, Materials & Continua*, vol. 9, pp. 253-280

Cheng, A. H. D.; Young, D. L.; Tsai, C. C. (2000): The solution of Poisson's equation by iterative DRBEM using compactly supported, positive definite radial basis function. *Engineering Analysis with Boundary Elements*, vol. 24(7), pp. 549-557.

Fairweather, G.; Karageorghis, A. (1998): The method of fundamental solutions for elliptic boundary value problems. *Advances in Computational Mathematics*, vol. 9, pp. 69-95.

Fu, Z. J.; Chen, W.; Yang, W. (2009): Winkler plate bending problems by a truly boundary-only boundary particle method. *Computational Mechanics*, vol. 44(6), pp. 757-763.

Fu, Z. J.; Chen, W. (2009): A truly boundary-only meshfree method applied to Kirchhoff plate bending problem. *Advances in Applied Mathematics and Mechanics*, vol. 1(3), pp. 341-352.

Han, Z. D.; Atluri, S. N. (2004): A Meshless Local Petrov-Galerkin (MLPG) Approach for 3-Dimensional Elasto-dynamics. *CMC: Computers, Materials & Continua*, vol. 1, pp. 129-140.

Hon, Y. C.; Wu, Z. M. (2000): Numerical computation for inverse determination problem. *Engineering Analysis with Boundary Elements*, vol. 24, pp. 599-606.

Karageorghis, A. (1992): Modified methods of fundamental solutions for harmonic and biharmonic problems with boundary singularities. *Numerical Methods for Partial Differential Equations*, vol. 8, pp. 1-19.

Li, S.; Liu, W. K. (2002): Meshfree and particle methods and their application. *Applied Mechanics Reviews*, vol. 55(1), pp. 1-34.

Liu, C. S. (2007a): A modified Trefftz method for two-dimensional Laplace equation considering the domain's characteristic length. *CMES: Computer Modeling in Engineering & Sciences*, vol. 21, pp. 53–66.

Liu, C. S. (2007b): A meshless regularized integral equation method for Laplace equation in arbitrary interior or exterior plane domains. *CMES: Computer Modeling in Engineering & Sciences*, vol. 19, pp. 99-109.

Liu, C. S. (2007c): A MRIEM for solving the Laplace equation in the doubly-connected domain. *CMES: Computer Modeling in Engineering & Sciences*, vol. 19, pp. 145-161.

Liu, C. S. (2008): Improving the ill-conditioning of the method of fundamental solutions for 2d Laplace equation. *CMES: Computer Modeling in Engineering & Sciences*, vol. 28, pp. 77–93.

Liu, C. S.; Yeih, W.; Atluri, S. N. (2009): On solving the ill-conditioned system $Ax = b$: general-purpose conditioners obtained from the boundary-collocation solution of the Laplace equation, using Trefftz expansions with multiple length scales. *CMES: Computer Modeling in Engineering & Sciences*, vol. 44, pp. 281-311.

Marin, L. (2008): Stable MFS solution to singular direct and inverse problems associated with the Laplace equation subjected to noisy data. *CMES: Computer Modeling in Engineering & Sciences*, vol. 37, pp. 203-242.

Marin, L. (2010a): Treatment of singularities in the method of fundamental solutions for two-dimensional Helmholtz-type equations. *Applied Mathematical Modelling*, vol. 34, pp. 1615-1633.

Marin, L. (2010b): A meshless method for the stable solution of singular inverse problems for two-dimensional Helmholtz-type equations. *Engineering Analysis with Boundary Elements*, vol. 34, pp. 274-288.

Ong, E. T.; Lim, K. M. (2005): Three-dimensional singular boundary elements for corner and edge singularities in potential problems. *Engineering Analysis with Boundary Elements*, vol. 29, pp. 175-189.

Poullikkas, A.; Karageorghis, A.; Georgiou G. (1998): Methods of fundamental solutions for harmonic and biharmonic boundary value problems. *Computational Mechanics*, vol. 21, pp. 416-423

Reutskiy, S.Y. (2005): The method of fundamental solutions for eigenproblems with Laplace and biharmonic operators. *CMC: Computers, Materials & Continua*, vol.2, pp.177-188.

Sarler, B. (2008): Chapter 15: Modified method of fundamental solutions for potential flow problems. Chen, C. S.; Karageorghis, A.; Smyrlis, Y. S. (ed.). *Method of Fundamental Solutions*. Dynamic Publisher.

Sladek, J.; Sladek, V.; Atluri, S. N. (2004): Meshless Local Petrov-Galerkin Method in Anisotropic Elasticity. *CMES: Computer Modeling in Engineering & Sciences*, vol.6, pp.477-490.

Smyrlis, Y. S.; Karageorghis, A. (2001): Some aspects of the method of fundamental solutions for certain harmonic problems. *Journal of Scientific Computing*, vol. 16, pp. 341-371.

Song, R. C.; Chen, W. (2009): A note on regularized meshless method for irregular domain problems. *CMES: Computer Modeling in Engineering & Sciences*, vol. 42, pp. 59-70.

Young, D. L.; Chen, K. H.; Lee, C. W. (2005): Novel meshless method for solving the potential problems with arbitrary domain. *Journal of Computational Physics*, vol. 209, pp. 290-321.

Young, D. L.; Chen, K. H.; Chen, J. T.; Kao, J. H. (2007): A modified method of fundamental solutions with source on the boundary for solving Laplace equations with circular and arbitrary domains. *CMES: Computer Modeling in Engineering & Sciences*, vol. 19, pp. 197-221.

Zienkiewicz, O. C.; Taylor, R. L. (1991): *The Finite Element Method* (Vol. 2), McGraw-Hill, New York.

